https://doi.org/10.21122/2227-1031-2024-23-5-417-426

UDC 629.331.03-83-592.3

Control Voltage Effect on Operational Characteristics of Vehicle Magnetorheological Damper

Le Van Nghia[1)], Dam Hoang Phuc[1)], Tran Trong Dat[1)], Nguyen Trung Kien[2)], S. V. Kharitonchik[3)], V. A. Kusyak[3)]

[1)]Hanoi University of Science and Technology (Hanoi, Socialist Republic of Vietnam),
[2)]Dai Nam University (Hanoi, Socialist Republic of Vietnam),
[3)]Belarusian National Technical University (Minsk, Republic of Belarus)

Abstract. Considering the increasingly large-scale application of magnetic fluids in various industries, we can confidently state that in the near future magnetorheological dampers will be widely used in adaptive automotive suspensions due to their operational flexibility and simplicity of controlling damping forces by changing the magnetic fluid properties according to parameters of surrounding electromagnetic field. The antivibration efficiency during operation is achieved by regulating the hydraulic resistance of the "magnetic" shock absorber by applying voltage to the windings of its coil. In addition to the physical properties of the oil used in the "magnetic" shock absorber, the viscosity of the working magnetorheological fluid is greatly influenced by the shape of the control signal. The paper focuses on the theoretical aspects of constructing a mathematical model of ac magnetorheological damper and presents the results of a computer experiment to assess effectiveness of its use as part of the adaptive suspension a passenger vehicle. In this case, the actual parameters of the "magnetic" shock absorber, used in modeling the dynamic process, were determined experimentally on a test bench, and the adequacy of the developed mathematical model was confirmed by the results of a semi-natural experiment. Using a verified model, the magnetorheological damper characteristics were obtained and compared for various forms of control signal, including rectangular voltage pulses of various frequencies and duty cycles, sinusoidal pulses and constant voltage signals. The analysis of the antivibration efficiency was carried out on the basis of the developed "quarter" model of a semi-active car suspension with a verified submo-del of a magnetorheological damper integrated into its structure. Moreover, the simulation scenarios were based on the selected strategy for controlling the voltage supplied to the windings of the "magnetic" shock absorber. As the results of theoretical and experimental studies have shown in terms of energy consumption, expansion of the working area of the damping characteristic and achieving smooth control of the damping force, the most effective is the use of a sinusoidal pulse voltage signal in the control circuit, which ensures a reduction in both the amplitude and damping time of oscillations. However, when de-signing and manufacturing a controller, creating a pulse modulator for generating sinusoidal pulses coinciding in phase and frequency with the vibrations of the car body is very difficult due to the random nature of external disturbances from the road surface. When a constant voltage is applied to the magnetorheological damper winding, the damping properties of the suspension are also improved compared to the basic design based on a traditional hydraulic shock absorber. Moreover, there is a proportional relationship between the voltage supplying the damper, the amplitude and damping time of the vibrations of the car body is observed. An increase in the control signal voltage from 1 to 2 V leads, in comparison with passive control of a magnetic shock absorber, to a decrease in the maximum amplitude of vibrations of the car body by 6.25 and 11.25 %, respectively, and a decrease in the vibration damping time by 0.72 and 1.41 s.

Keywords: active automotive suspension, magnetorheological damper, ¼ car suspension model; Dahl model, control voltage signals, semi-natural experiment, magnetorheological damper testing, simulation, damping characteristics

For citation: Nghia Le Van, Phuc Dam Hoang, Dat Tran Trong, Kien Nguyen Trung, Kharytonchyk S. V. , Kusyak V. A. (2024) Control Voltage Effect on Operational Characteristics of Vehicle Magnetorheological Damper. *Science and Technique*. 23 (5), 416–425. https://doi.org/10.21122/2227-1031-2024-23-5-416-425

Адрес для переписки
Дам Хоанг Пхук
Ханойский университет науки и технологий
ул. Дай Ко Вьет, 1,
100000, г. Ханой, Вьетнам
Тел.: +84 932367577
Hoan.nguyentrong@hust.edu.vn

Address for correspondence
Dam Hoang Phuc
Hanoi University of Science and Technology
1, Dai Co Viet Street,
100000, Ha Noi, Viet Nam
Tel.: +84 932367577
Hoan.nguyentrong@hust.edu.vn

Влияние управляющего напряжения на эксплуатационные характеристики магнитореологического демпфера автомобиля

Ле Ван Нгиа[1)], Дам Хоанг Пхук[1)], Чан Чонг Дат[1)], Нгуен Чунг Кьен[2)], С. В. Харитончик[3)], В. А. Кусяк[3)]

[1)]Ханойский университет науки и технологий (Ханой, Социалистическая Республика Вьетнам),
[2)]Дай Нам университет (Ханой, Социалистическая Республика Вьетнам),
[3)]Белорусский национальный технический университет (Минск, Республика Беларусь)

Реферат. Учитывая все более масштабное применение магнитных жидкостей в различных отраслях промышленности, можно с уверенностью констатировать, что в ближайшем будущем магнитореологические демпферы будут широко использоваться в автомобильных подвесках адаптивного класса ввиду их эксплуатационной универсальности и несложного алгоритма управления энергией рассеивания при изменении свойств магнитной жидкости в зависимости от параметров электромагнитного поля. Эффективность гашения колебаний в процессе движения достигается за счет регулирования гидравлического сопротивления «магнитного» амортизатора посредством подачи напряжения на обмотки его катушки. Помимо физических свойств используемого в «магнитном» амортизаторе масла, на вязкость рабочей магнитореологической жидкости большое влияние оказывает форма управляющего сигнала. В статье рассматриваются теоретические аспекты построения математической модели магнитореологического демпфера и приводятся результаты компьютерного эксперимента по оценке эффективности его использования в составе адаптивной подвески легкового автомобиля. При этом фактические параметры «магнитного» амортизатора, используемые при моделировании динамического процесса, определялись экспериментально на испытательном стенде, а адекватность разработанной математической модели подтверждена результатами полунатурного эксперимента. С помощью верефицированной модели получены и сопоставлены характеристики магнитореологических демпферов при различных формах управляющего сигнала, включая прямоугольные импульсы напряжения различной частоты и коэффициента заполнения, синусоидальные импульсы и сигналы постоянного напряжения. Анализ эффективности гашения колебаний проводился на базе разработанной «четвертной» модели полуактивной подвески автомобиля с интегрированной в ее структуру верифицированной субмоделью магнитореологического демпфера. Причем сценарии моделирования основывались на выбранной стратегии управления напряжением, подаваемым на обмотки «магнитного» амортизатора. Как показали результаты теоретических и экспериментальных исследований с точек зрения энергопотребления, расширения рабочей области демпфирующей характеристики и достижения плавности управления демпфирующей силой, наиболее эффективным является использование в цепи управления синусоидального импульсного сигнала напряжения, обеспечивающего уменьшение как амплитуды, так и времени гашения колебаний. Однако при проектировании и изготовлении контроллера создание импульсного модулятора, генерирующего синусоидальные импульсы, совпадающие по фазе и частоте с колебаниями кузова автомобиля, весьма затруднительно ввиду случайного характера внешних возмущений от дорожного покрытия. При подаче на обмотку магнитореологического демпфера сигнала постоянного напряжения демпфирующие свойства подвески также улучшаются по сравнению с базовой конструкцией на основе традиционного гидравлического амортизатора. Причем прослеживается пропорциональная зависимость между вольтажом питающего демпфер напряжения, амплитудой и временем затухания колебаний кузова автомобиля. Увеличение напряжения управляющего сигнала с 1 до 2 В приводит по сравнению с пассивным управлением магнитным амортизатором к снижению максимальной амплитуды колебаний кузова автомобиля соответственно на 6,25 и 11,25 % и уменьшению времени гашения колебаний на 0,72 и 1,41 с.

Ключевые слова: активная подвеска автомобиля, магнитореологический демпфер; модель 1/4 подвески автомобиля; модель Даля, сигналы управляющего напряжения, полунатурный эксперимент, испытание магнитореологического демпфера, имитационное моделирование, характеристики демпфирования

Для цитирования: Влияние управляющего напряжения на эксплуатационные характеристики магнитореологического демпфера автомобиля / Ле Ван Нгиа [и др.] // *Наука и техника.* 2024. Т. 23, № 5. С. 417–426. https://doi.org/10.21122/2227-1031-2024-23-5-417-426

Introduction

Due to the unique properties of magnetorheological (MR) fluids the last one has been used in a wide variety of applications such as rotary brakes, forging equipment, clutches, polishing and grinding equipment [1–6]. Among them, MR liquid dampers are semi-active control devices that are widely used in today's industrial applications. Magnetic rheological damper (MRD) is one of the semi-active devices that promises to be commonly used in automotive engineering. The main feature of MRD is magnetic rheological oil, whose specific properties can be changed by applying a magnetic field, which in turn can leads to inducing force variation in the damping [7, 8].

To study the model of the MR damper, several methods have been proposed over the years to obtain MR damper models and determine their parameters. Spencer and colleagues [9] developed a phenomenological model that accurately describes the response of MR dampers to cyclic stimuli. This is a modified Bouc–Wen (BW) model adjusted by ordinary differential equations. The models based on the BW in semi-active seismic vibration control have proven to be easy in usage and have an acceptable quantity. Using a different approach from Spencer's, Kyle et al modeled an MR damper as a Takagi–Sugeno–Kang fuzzy inference system [10]. The model's training and test data were generated using Spencer's MR damper model.

In a study at Sakarya University, experimental and theoretical analysis was performed to predict the behavior of a linear rheological magnetic damper. A rheological magnetic damper was designed and built for dynamic testing on a mechanical cage that sinusoidal stimulus. The same flow analysis was performed on the prototype MR damper based on the Bingham model, and a parametric algebraic model was analyzed to test the hysteresis behavior of the MR damper. The final observation was that the algebraic model succeeded at the highest excitation velocity of 0.2 m/s [11].

Other authors have studied the response of the MR damper, emphasizing the difference between the pre-elastic and the posterior viscous volumes as an essential aspect of the damper. The study by Spencer, Butz, and Stryk showed that the difference between using the modified BW model and the Bingham-plastic model in a 2-degree-of-freedom automotive dynamic system was minimal [12].

In 2003, John Gravatt conducted a performance test of the suspension combined with the MR shock absorber on a sports motorcycle. The obtained results showed the criterion of reducing suspension displacement, stability time, and oscillation of the suspension system when equipped with MR dampers, thereby improving the efficiency in reducing instability [13].

Due to their enormous force control ability, magnetic rheological dampers have been used to avoid seismic effects caused by earthquakes on civil works. In an experiment, the dynamic power of the damper checked by a dynamic excitation test was compared with two types of rheological fluids. Two types of rheological fluids are 132LD, manufactured by Lord Corporation, and experimental product #104, manufactured by Bando Chemical Industries on a trial basis [14].

Like the above experiment, an MR liquid sample was developed using OKS1050 silicone oil and mixed with carbonyl powder. Furthermore, to reduce deposition, Aerosi200 was added as a stabilizer, and the finite element method modeled the magnetic field acting on the rheological liquid. Then the model was analyzed by ANSYS software, and the results showed that the model completely satisfied the dynamic characteristics of the mechanical system [10].

Kyle and Roschke used a fuzzy logic-based model with three inputs: displacement, voltage, and velocity, which were modeled on the data generated by the simulation. From the experimentally measured data, it can be seen that the hysteresis loop is independent of the steady field. Therefore, the BW model parameters are considered independent of the current [15].

According to the research [16], the controlled damping force was generated depending on the control current. In addition, MR fluid shock absorbers were operated with high reliability, and their functions were virtually uninterrupted by temperature fluctuations or any impurities in the fluid. However, the significant disadvantage hindering the MR fluid damper was its non-linear properties concerning force versus displacement and hysteresis force versus velocity. Therefore, making an MR fluid damper with maximum efficiency is a big challenge, especially when it comes to making an accurate model to take full advantage of this particular device. Another is to design the most efficient algorithm to improve the system's performance.

The MRD characteristic is a function of the voltage or current flowing into the solenoid coil. In addition, this characteristic is highly dependent on the input voltage or current characteristics. Thanks to this relationship, the drag coefficient of the MR dampers can be easily controlled in real-time. Therefore, the study of MR damping is necessary, which requires studies in building MR damping models.

This article presents a study on the influence of voltage-controlled signals on the characteristics of MR dampers, thereby providing a basis for developping control algorithms for car’s active suspension systems. A simulation method combined with experiments is chosen to conduct the research.

Specifically, an MR damper model is constructed and validated through experiments on a test bench. This model is then used to develop a quarter-car suspension system model, analyzing the effectiveness of MR dampers when the vehicle encounters road irregularities.

System design and results

Suspension model combined with MR shock absorber. The MR damper has a non-linear characteristic curve, which makes it difficult to describe its behavior. The proposed models must be accurate, that is, the output of the predictive model and the experimental data must be the same. The model must also be simple to allow an easy parameter identification, and the controls are less complex and ultimately reversible, meaning that different inputs and outputs can be selected and changed position.

In 1968 the magnetic field damping model was independently proposed by Dahl to describe friction behavior and developed by Bouc (1971) to represent hysteresis phenomena. Dahl's viscous model used in this study is based on the model proposed by Aguirre [17]. The diagram of Dahl's viscous model is shown in Fig. 1.

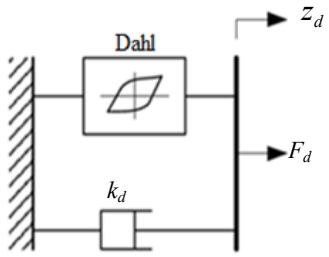

Fig. 1. Dahl model diagram

Dahl's MR damping model, described by equations (1) and (2), considers semi-static links in the origin of friction. The damping force F_d is a function of the instantaneous damper piston velocity $\dot{z}_d$. In addition, the damping force F_d is also affected by the hysteresis loop shape parameters k_d, k_{wa}, k_{wb}, ρ and the dynamic hysteresis coefficient w, describing the nonlinear damping behaviour:

$$F_d = k_d \dot{z}_d + \left(k_{wa} + k_{wb} u\right) w; \qquad (1)$$

$$\dot{w} = \rho\left(\dot{z}_d - \left|\dot{z}_d\right| w\right), \qquad (2)$$

where u – MRD coil control voltage, V.

From equation (2), it can be shown that increasing the voltage u or k_{wb} will have the same effect on the shape. Increasing either of them will result in an increase in the value in the hysteresis loop. Reducing ρ will change the width of the hysteresis ring, producing a rapid change in force. The hysteresis parameters, used in the Dahl's viscous model are the following: u = 0.3 V, k_d = 5, k_{wa} = 80, k_{wb} = 80, ρ = 10.

Car's ¼ suspension model combined with MR shock absorber is shown on Fig. 2, where the passive damping element is replaced by MR damper and the damping coefficient c_s is no longer shown. The right part is the MR shock absorber; the left one is the passive 1/4 suspension model. The input of the 1/4 suspension model is the road surface vibration z_r (the study uses the 5 cm square pulse-shaped pavement impact) and the magnetic damping force F_d of MR shock absorber. The output of the model is the vehicle body displacement z_b, the wheel displacement z_w, and the oscillation body velocity $\dot{z}_d$, which is the input of the MR damping model. As a result, the suspension system has only two parameters, k and F_d (F_d: MR damping force calculated using the Dahl model).

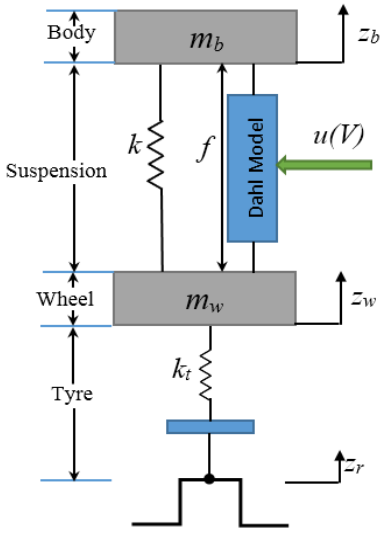

Fig. 2. Car's ¼ suspension model with MR damper
k, k_t – stiffness of the spring element and tire, k = 12500 N/m, k_t = 76000 N/m ; m_b, m_w – vehicle body and wheel weights, m_b = 342 kg, m_w =38 kg; F_d – MRD damping force, N

Equation (1) combined with MR damping gives the following equation:

$$\begin{cases} m_b \ddot{z}_b = -k(z_b - z_w) + F_d; \\ m_w \ddot{z}_w = k(z_b - z_w) - k_t(z_w - z_r) - F_d, \end{cases} \qquad (3)$$

where $\ddot{z}_b$, $\ddot{z}_w$ – accelerations of the sprung and unsprung masses.

Experimental determination of Dahl model parameters and experimental results. For experimental determination of damping characteristics a special test bench (Fig. 3) was manufactured at Department of Automotive Engineering group of Hanoi University of Science and Technology.

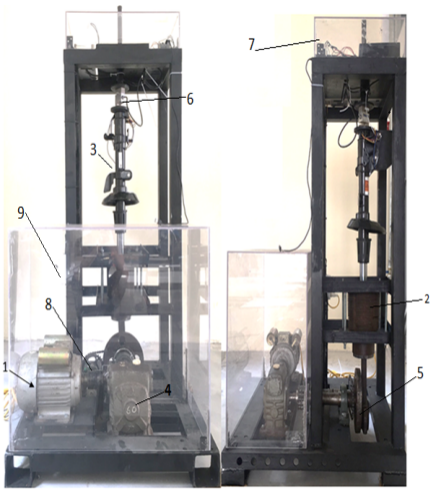

Fig. 3. Test equipment for damping characteristics
1 – Motor; 2 – Cylinder-piston; 3 – MR damper; 4 – Gearbox;
5 – Eccentric disc; 6 – Force sensor (load cell);
7– Control box; 8 – Pulse encoder; 9 – Power switch

Test equipment includes BWI front suspension MR damper 3 (see Fig. 3) of Acurra 2011 cars, which has the following characteristics:

– Dimensions, $L \times D \times d$: 760×287×259 mm.

– Weight: 3,1 kg.

– The change in damping force with the expression variations from 0 to 1 V: about 800 N.

– Inner solenoid coil resistance of damper measured: 1 Ω at 29 °C.

In this study, damping characteristics were measured at low voltage supply states. The test scenario involves measuring the force acting on the piston, piston rod displacement/velocity and the encoder pulse when the control voltage changes from 0 to 1 V with an average step of 0.2 V [18].

The comparison of MR damping properties between simulation and experiment through qualitative geometry is shown in Fig. 4. The graph shows damping characteristics based on the relationship between the force-velocity and the force-displacement of the piston under the action of a voltage of 0.1 V.

According to the graph, regarding the profile of the force-displacement relationship, the damping force is symmetrical about the axis. Do the same for different supply voltages to the damper, thereby building a relationship between the hysteresis parameter values on the Dahl model and the control voltage.

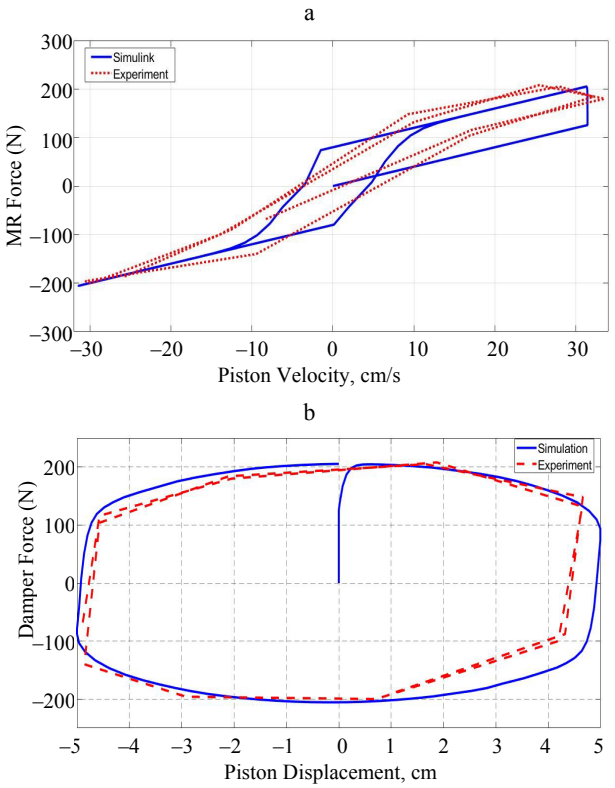

Fig. 4. Simulation and experiment damping characteristics when applying voltage 0.1 V:
a – Force-velocity characteristic of MR damping;
b – Force-displacement characteristic of MR damping

Qualitatively, the characteristics of the damping force according to the simulation are close to the characteristic curve when experimenting, which shows that the parameters used in the simulation are very close to the actual conditions. These parameters were evaluated and determined through the correlation function to find the ratio between simulation and experiment by determinng the force at the same displacement position on the graph. The summary and evaluation of the correlation between simulation according to the Dahl model and MR Acurra 2011 damping experiment is shown in Table 1.

Thus, the correlation coefficient between the simulation and experiment is close to 1, which can be concluded that the parameters used in the simulation are relatively consistent with the actual experimental determination of MR damping characteristics using the 2011 Acurra front suspension.

This parameter will be used to simulate the characteristics of the MR dampers under the influence of different voltages.

Table 1

Correlation between simulation and experiment

Voltage (V)	Correlation between simulation and experiment
0	0,9831
0.1	0,9693
0.3	0,9782
0.5	0.9841
0.8	0.9263
1.0	0.9657

Simulation of MR damping performance. To study the influence of control signal form on the characteristics of MR dampers, the paper uses the Dahl's model with different control voltage signals, schematically depicted in Fig. 5.

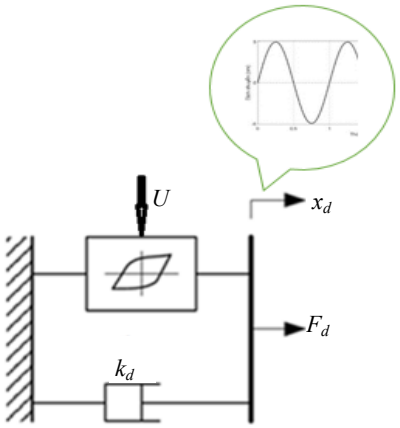

Fig. 5. Schematic simulation of the voltage effect on MRD damping characteristics

In this diagram, the x_d displacement signal is a sine wave with the amplitude of 5 cm and the frequency of 1 Hz. The control input voltage signal for the MR damper is the voltage signal U. This voltage varies according to the preselected characteristics and is shown in Table 2 [19].

Table 2

MR. damping characteristic simulation scenario

Alternative	Control Voltage	Characteristic
1	Constant voltage level 0 and 0.5 V	Force-time ($F_d - t$)
2	Sine and square pulse voltage supply, positive side, 0.5 V amplitude	Force-displacement ($F_d - z_d$)
3	Sine and square pulse voltage supply, negative-positive symmetry, 0.5 V amplitude	Force-velocity ($F_d - \dot{z}_d$)

In case of constant voltage supply 0 and 0.5 V to the MR damper (see Table 2, alternative 1) the simulation results of the damping characteristics are shown in Fig. 6 and 7. The graphs show the time history of MR damping force characteristics, according to velocity and piston displacement.

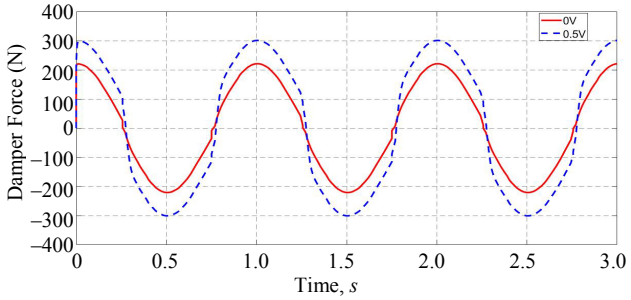

Fig. 6. $F_d - t$ characteristic at a constant control voltage

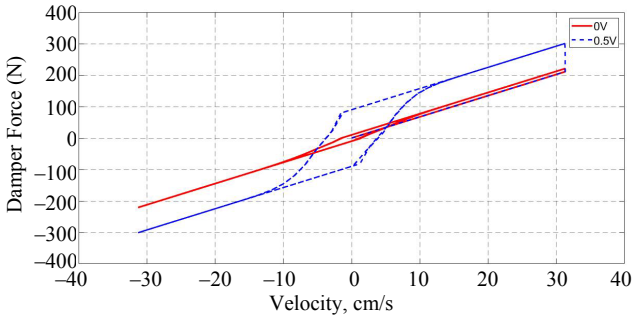

Fig. 7. $F_d - \dot{z}_d$ characteristic at a constant control voltage

According to Fig. 6, when the constant voltage is applied to the shock absorber, the damping force has the same profile as the velocity (faster than the displacement z_d by $\pi/2$). This shows that MR dampers' characteristics are similar to those of passive dampers ($F_d \cdot \dot{z}_d > 0$). However, the value of the damping force is proportional to the input voltage; the profile is also steeper when increasing the control voltage ($F_d - t$ graph), showing a very immediate effect on the damping when the voltage is present. In Fig. 7 ($F_d - \dot{z}_d$ graph), in the state without controlling voltage, the damping characteristic is almost the same as that of the passive damping type (the characteristic curve is quite linear); however, when the controlling voltage is applied, in the input control, the damping force varies significantly for the low-speed, while in the high-speed, the damping force has a linear characteristic. This shows that with a constant control voltage, the damping force with velocity ($F_d - \dot{z}_d$) characteristic divides into two zones:

– low-speed zone: the area with high hysteresis; the applied force significantly differs between the compression and return strokes;

– high-velocity zone: the force characteristics have almost no hysteresis; the force value increases linearly with the speed and damper input voltage.

In case of positive side voltage pulse supply to the MR damper (see Table 2, alternative 2) – the simulation results of the damping characteristics under two pulse types *"sine"* and *"square"* are shown in Fig. 8 and 9 through 2 graphs: $F_d - t$ and $F_d - \dot{z}_d$.

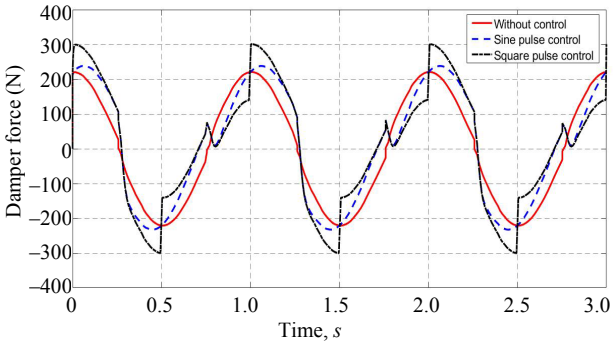

Fig 8. $F_d - t$ characteristic at positive side control voltage

On the graph ($F_d - t$) (Fig. 8), the oscillation phase of the force is still in phase with the piston speed, but the force amplitude is small and the damping force characteristics between the two control pulses are very close together. At some point on the force curve when driven by a *"square"* pulse, the damping force has a characteristic stepwise step over the pulse duration (in locations where the control voltage is sudden, the force spikes sudden), this will affect the smoothness of the body. After a short time, this force characteristic coincides with the force characteristic of the *"sine"* impulse control pulse. This shows that the sine control signal will give better controllability and energy saving than the square pulse signal.

The force versus velocity characteristics is shown in Fig. 9. The graph ($F_d - \dot{z}_d$) shows that the hysteresis area of the damping force is extended to include the high-velocity zone, overcoming the disadvantage compared to the control in the form of constant voltage. The hysteresis area of the damping force in two different compression and return states is more comprehensive when the damping is in the compressed state. It shows that the shock absorber has a wider working area in the compression state with this control pulse.

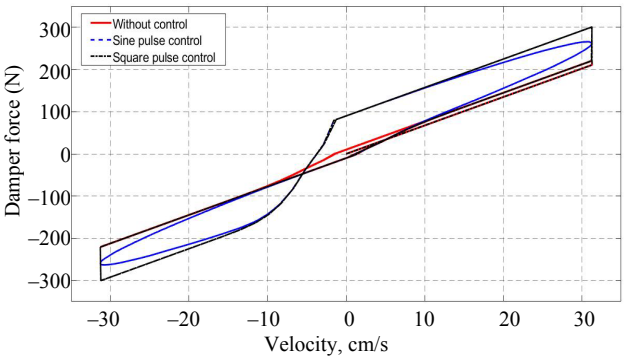

Fig. 9. $F_d - \dot{z}_d$ characteristic at positive side control voltage

In case of positive-negative symmetrical voltage pulse supply to the MR damper (see table 2, alternative 3) the simulation results of the damping characteristics are shown in Fig. 10 and 11.

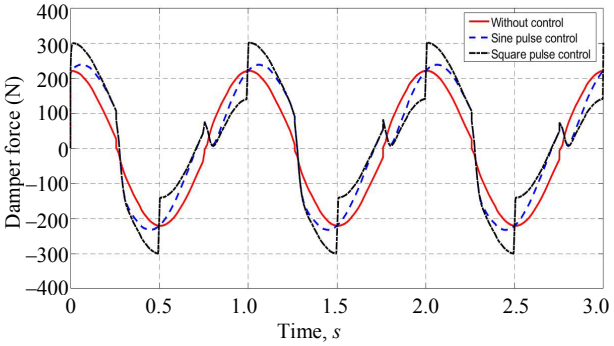

Fig. 10. $F_d - t$ characteristic at positive-negative symmetrical control voltage

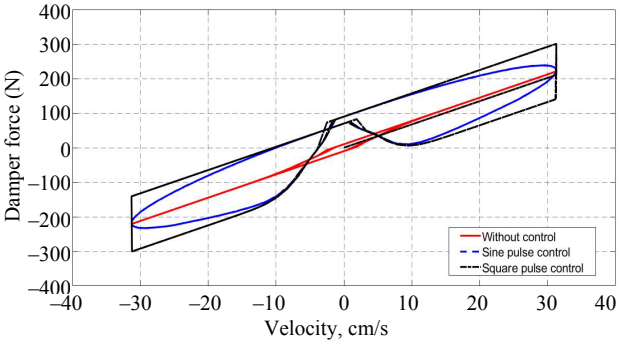

Fig. 11. $F_d - \dot{z}_d$ characteristic at positive-negative symmetrical control voltage

The amplitude of the maximum force is reduced in the case of *"sine"* pulses and unchanged in the *"square"* case, besides, the force profiles in the two cases appear with many jumping points. For *"square"* pulses are points where the supply

voltage direction changes, while *"sine"* pulses are points with extremes on the "negative" side, the force characteristics ($F_d - t$) when driven by a *"square"* pulse for the jump larger than the *"sine"* pulse.

On the ($F_d - \dot{z}_d$) graph, the hysteresis zone of the force is also enlarged, as in the case of positive flank impulse supply.

Comment: The damping force characteristics are various with different types of control voltages. With a constant control voltage, the force drop is symmetrical both in the compression and the release strokes and have a smooth curved characteristic, the slope of which changes with the input voltage. In the two cases of the pulse voltage supply, it was found that the damping is more effective in the compression stroke, which allows the control voltage characteristic to be developed when designing the control for this type of damping, thereby helping to extend its operational tuning range relative to an initially specified control characteristic.

In this simulation range, the impulse control voltage signal is fed according to the piston oscillation frequency, so according to the results in Fig. 8 and 9, the positive side "sine" pulse level is the best based on the damping force and power characteristics for control. Because, with this type of control pulse, the curvilinear force characteristic is smooth, without a jump, the damping hysteresis zone is widened to the high-velocity region. In addition, according to the power supply criterion, this type of control is energy saving one because the average voltage is lower than in case of the control with constant voltage.

However, when designing and manufacturing a controller, a pulse modulator controlled by a *"sine"* pulse coinciding with vehicle body oscillations (phase and frequency) will be difficult when the pavement excitations are random and unpredictable. That will increase the cost of the control system, therefore, the study selects the damping control voltage as constant over time.

Simulation of suspension system with MR damper. In the scope of the research, the paper uses the 5 cm square pulse-shaped pavement impact (see Fig. 2) to examine the response of the suspension system to the vibration of the vehicle body under the effect of different MR shock absorber input voltage values. The study uses the Dahl model coupled with the a quarter car suspension model to evaluate the effectiveness of MR shock absorbers arranged in the suspension system. The evaluation criterions are the maximum vibration amplitude of the vehicle body and the oscillations quenching time [20]. The simulation strategy is shown in Table 3, the simulation results are presented in Fig. 12 and 13.

Table 3

Simulation scheme of operation suspension system with MR damper

Alternative	Input	Voltage (V)	Evaluation criteria
1	Square pulsating road surface undulation	0	Amplitude, body oscillation frequency, oscillations quenching time
2		1	
3		2	

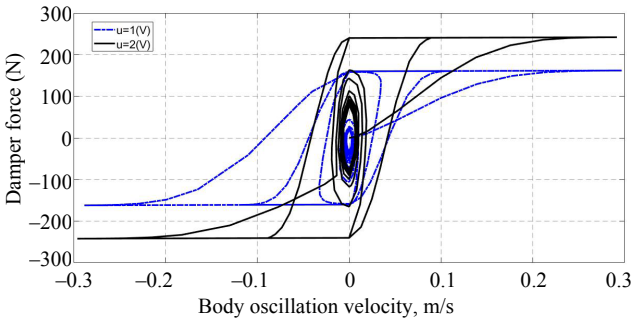

Fig. 12. $F_d - \dot{z}_d$ characteristics on suspension with MR dampers

According to the $F_d - \dot{z}_d$ graph, the damping force also increases when the damper input voltage increases. The damping force increases depending on the piston rod's speed and the voltage applied to the damper. The higher the voltage is, the smaller the oscillation amplitude of the vehicle body and the smaller the oscillation time becomes.

The results of body oscillation are shown in Fig. 13. The effect of suppressing the vibrations of the vehicle's body when there is a control current in the dampers is much higher than when there is no control.

The maximum amplitude of oscillation of the vehicle body when the voltage level is larger, the greater the amplitude and damping time reductions. Specifically, in comparison with the passive damper, when the voltage control level is 1 and 2 V, the reduction of maximum amplitude is 6.25 and 11.25 %, and the damping time reduction

is 0.72 and 1.41 s respectively. With a small control voltage, the amplitude of the oscillation is reduced, but the oscillation time is still ample. The more the control current, the higher the ability to extinguish the oscillation, both in amplitude and time. It shows the vibration-suppressing efficiency of the MR dampers in the car's 1/4 suspension model.

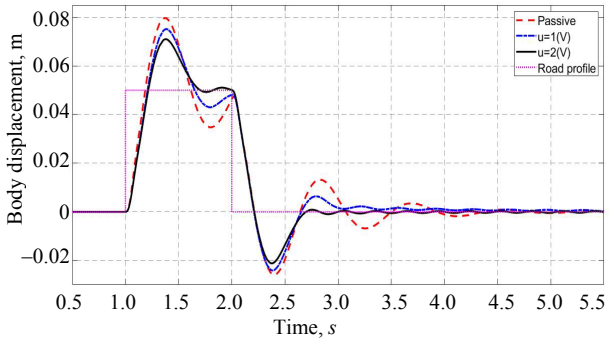

Fig. 13. Body displacement comparison

When no current is applied to the shock absorber, the damping force is not zero. The MR shock absorber acts as a passive shock absorber because the viscosity of the liquid is also the cause of the damping effect when the damping is in the off state.

CONCLUSION

The study presented the magnetorheological damper model for determining the characteristics of MR dampers. The damper test bend was built to measure the force-velocity and the force-displacement characteristics of the vehicle damper piston and to verify the accuracy of the proposed model. The correlation between the simulation result and experiment data is greater than 0.92, which shows a high level of proposed model reliability. This verified model was used to develop the 1/4 semiactive suspension car model for evaluation of the vibration efficiency.

The study investigated the characteristics of MR dampers under the effect of different control signals, and the simulation results showed that the MR damping control achieved the most optimal efficiency using a "sine" control signal. The positive side has a control frequency that coincides with the characteristics of the input oscillation. However, it is challenging to design a control pulse generator in the form of a sine pulse whose frequency coincides with the oscillation frequency of the vehicle body. Therefore, in the study, the control signal type is selected as a constant voltage form because it ensures both the working efficiency of the dampers and the simplicity of the control circuit design.

In addition, the study also focuses on simulating the integrated model of a quarter car suspension system with MR dampers, simulating and investigating the efficiency of vibration suppression controlled by the constant voltage. Specifically, a quarter car has MR dampers with 1 and 2 V control voltage. The evaluation of the vibration suppression efficiency through comparison of body displacement shows the effectiveness of MR dampers in suppressing vibrations of the suspension system. As the voltage level increases, the maximum amplitude of the vehicle body's oscillation becomes greater, leading to a reduction in both amplitude and damping time. Specifically, in comparison with the passive damper, when the voltage control level is 1 and 2 V, the reduction of maximum amplitude is 6.25 and 11.25 %, and the damping time reduction is 0.72 and 1.41 s respectively.

From the above results, the user can control the damping force of the MR damper by varying the input supply voltage or current to the magnetic coil. It is necessary for algorithm research and developing semi-active suspension control with MR dampers.

Funding: This research is funded by the Hanoi University of Science and Technology under project number T2023-PC-023.

REFERENCES

1. Hoang Quang Tuan, Trinh Minh Hoang (2023) Simulation-Based Investigation of the Effects of Major Parameters on Magnetorheological Brake Torque. *Journal of Southwest Jiaotong University* 58 (3), 244–251. https://doi.org/10.35741/issn.0258-2724.58.3.21.
2. Hoang Q. T., Trinh M. H., Nguyen N. A., Tran T. T. Determination of Magnetorheological Brake Characteristics by Experiment on the Test Rig. *Proceedings of the 3rd Annual International Conference on Material, Machines and Methods for Sustainable Development (MMMS2022)*. Lecture Notes in Mechanical Engineering. Springer. Cham. https://doi.org/10.1007/978-3-031-31824-5_47.

3. Song W.-L., Li D.-H., Tao Y., Wang N., Xiu S.-C. (2017) Simulation and Experimentation of a Magnetorheological Brake with Adjustable Gap. *Journal of Intelligent Material Systems and Structures*. 28 (12), 1614–1626. https://doi.org/10.1177/1045389X16679022.
4. Agyeman P. K., Tan G., Alex F. J., Peng D., Valiev J., Tang J. (2021) The Study on Thermal Management of Magnetorheological Fluid Retarder with Thermoelectric Cooling Module. *Case Studies in Thermal Engineering*, 28, 101686. https://doi.org/10.1016/j.csite.2021.101686.
5. Bashtovoi V., Reks A., Motsar A. (2017) Energy Dissipation in A Finite Volume of Magnetic Fluid. *Journal of Magnetism and Magnetic Materials*, 431, 245–248. https://doi.org/10.1016/j.jmmm.2016.08.025.
6. Bashtovoi V., Reks A., Motsar A., Vikulenkov A. V., Klishev O. P., Markachev N. A., Sel'kov D. A., Tikhonov V. A., Uspenskii E. S. (2014) *Magnetic Fluid Dynamic Vibration Damper.* Patent BY 18250 (in Russian).
7. Lord Corporation Engineering note (1999) *Designing with MR Fluids.* Lord Corporation Engineering note, Thomas Lord Research Center, Cary, NC, December 1999.
8. Yuan X., Tian T., Ling H., Qiu T., He H. (2019) A Review on Structural Development of Magnetorheological Fluid Damper. *Shock and Vibration*, 2019, 1498962. https://doi.org/10.1155/2019/1498962.
9. Spencer B. F., Dyke S. J., Sain M. K., Carlson J. D. (1997) Phenomenological Model for Magnetorheological Dampers. *Journal of Engineering Mechanics*, 123 (3), 230–238. https://doi.org/10.1061/(asce)0733-9399(1997)123:3(230).
10. Schurter K. C., Roschke P.N. (2000) Fuzzy Modelling of a Magnetorheological Damper Using ANFIS. *IEEE International Conference on Fuzzy Systems*. San Antonio, Texas, USA, 122–127. https://doi.org/10.1109/fuzzy.2000.838645.
11. Butz T., von Stryk O. (1999) *Modelling and Simulation of Rheological Fluid Devices*. Preprint SFB-438-9911. Technische Universität München, Germany.
12. Şahin İ., Engin T., Çeşmeci Ş. (2010). Comparison of Some Existing Parametric Models for Magnetorheological Fluid Dampers. *Smart Materials and Structures*, 19 (3), 035012. https://doi.org/10.1088/0964-1726/19/3/035012.
13. Fujitani H., Sakae H., Kawasak, R., Fujii H., Hiwatashi T., Saito T. (2008). Verification of Real-Time Hybrid Tests of Response Control of Base Isolation System by MR Damper Comparing Shaking Table Tests. *Sensors and Smart Structures Technologies for Civil, Mechanical, and Aerospace Systems 2008*, 6932, 264–272. https://doi.org/10.1117/12.791079.
14. Kciuk M., Kurc A., Szewczenko J. (2010). Structure and Corrosion Resistance of Aluminium AlMg2. 5; $AlMg_5Mn$ and AlZn5Mg1 alloys. *Journal of Achievements in Materials and Manufacturing Engineering*, 41 (1/2), 74–81.
15. Coulter J. P., Weiss K. D., Carlson J. D. (1993) Engineering Applications of Electrorheological Materials. *Journal of Intelligent Material Systems and Structures*, 4 (2), 248–259. https://doi.org/10.1177/1045389x9300400215.
16. Eshkabilov S. L. (2017) Modeling and Simulation of Non-Linear and Hysteresis Behavior of Magneto-Rheological Dampers in the Example of Quarter-Car Model. *International Journal of Theoretical and Applied Mathematics,* 2 (2), 170–189. https://doi.org/10.11648/j.ijtam.20160 202.32.
17. Aguirre Carvajal N., Ikhouane F., Rodellar Benedé J., Wagg D., Neild S. (2010) Viscous + Dahl Model for MR Dmper Characterization: A Real-Time Hybrid Test (RTHT) Validation. *14th European Conference on Earthquake Engineering 2010.* Ohrid, Republic of Macedonia, 30 August-3 September 2010. Available at: https://eprints.whiterose.ac.uk/96083/1/14ECEE_Naile%20Aguirre_1023.pdf.
18. Agrawal A., Kulkarni P., Vieira S. L., Naganathan N. G. (2001) An Overview of Magneto- and Electro-Rheological Fluids and Their Applications in Fluid Power Systems. *International Journal of Fluid Power*, 2, 5–36. https://doi.org/10.1080/14399776.2001.10781106.
19. Rabinow J. (1948) The Magnetic Fluid Clutch. *Transactions of the American Institute of Electrical Engineers,* 67 (2), 1308–1315. https://doi.org/10.1109/t-aiee.1948.5059821.
20. Butz T. (1999) *Parameter Identification in Vehicle Dynamics*. Diploma Thesis, Zentrum Mathematik, Technische Universität München.

Received: 18.06.2024
Accepted: 20.08.2024
Published online: 30.09.2024